

ASSESSMENT OF SANDWICH BEAMS WITH RIGID POLYURETHANE FOAM CORE USING FAILURE-MODE MAPS

Emanoil LINUL, Liviu MARŞAVINA

“Politehnica” University of Timisoara, Department of Mechanics and Strength of Materials, 1 Mihai Viteazu Avenue, 300 222
Timisoara, Romania
E-mail: linul_emanoil@yahoo.com

The failure-mode maps of composite sandwich beams can provide useful information about the influence of different design parameters on the failure behaviour of such components. Failure mode of sandwich beams with different cores and different faces were investigated in the experimental program. Foams with 40 and 200 kg/m³ densities were used as core material, while Glass-Fibre Reinforced Polymer (GFRP), polyester, epoxy and aluminium are the faces materials. Three-point bending tests were carried out for sandwich beams. In order to characterize these sandwich materials first were carried out a statistical analysis of the cellular structure for two different densities of the core material above mentioned. The sandwich core morphology and cells dimensions were studied before testing through scanning electron microscopy (SEM) and pore diameter versus frequency of pores histogram were plotted. After statistical analysis were performed static compression tests. These compression tests have had as objective the determining of the main mechanical properties such as Young's modulus and yield stress values. The results obtained from the static compression tests were used for the analytical determination of failure-mode maps of sandwich beams. Finally, the failure-mode maps were constructed for five considered sandwich types and validated by the experimental results. Each failure-mode map is characteristic for a family of sandwich beam designs.

Key words: sandwich beam, polyurethane foams, failure-mode maps, three-point bending tests.

1. INTRODUCTION

Composite structural members made of two thin, stiff faces separated by a weak, light-weight core are known as sandwich panels. Separation of the stiff faces by the core increases the moment of inertia of a sandwich beam or plate with little increase in weight, enhancing the properties in bending and buckling. Sandwich structures are widely used because of its ability to provide high bending moment stiffness coupled with light weight. Because of this, sandwich panels are often used in applications where weight-saving is critical: in aviation applications in recent years for flooring, helicopter rotor blades, and tail and wing components. Panels for aircraft structures almost invariably employ fibre composite faces with metal or paper-resin honeycomb or corrugated [1–4]. Their good energy absorbance combined with high flexural rigidity, furthermore makes them ideal for the manufacture of large panels and modern sports equipment: the decks and ship hulls of racing yachts, and water and snow skis [5–9]. Also, the automobile industry is beginning to use the concepts developed by the aircraft industry for sandwich construction in the cars of the future. In the non-residential building market sandwich panel roofing is gaining increasing popularity because of its low weight. Other constructions applications include: portable buildings and fold-up bridges (of potential use to the Army) [1].

In most applications the panel must have some required minimum stiffness, it must not fail under some maximum service loading and it must be as light as possible. Its design can be formulated as an optimization problem: the goal is the panel with minimum weight which meets the requirements for stiffness and strength. The optimization can be carried out with respect to the: core and skin dimensions, the core and skin materials and to the core density. The obvious attraction of sandwich structures is that they are light and stiff. But stiffness is not enough. The beam or panel must also have strength: it must carry the design loads without failing. At least five different failure modes are possible; a given sandwich will fail by the one which occurs

at the lowest load, and as the geometry and loading change the failure mode can change, too. So it is not enough to design against one mode; all must be considered, and the dominant mode—the one which determines failure—identified and evaluated [1, 2]. A potentially useful tool for design of sandwich structures is the concept of a failure mode map, where the failure modes are identified as a function of the design variables such as face and core and structure dimensions, and the core and the face material properties [10].

2. FAILURE-MODE MAPS OF SANDWICH BEAMS LOADED IN THREE POINT BENDING

As has been mentioned above, sandwich beam or panel can fail in several ways. It may fail by the yielding or fracture of the faces [11–15]. The compression face may “wrinkle” – a local buckling of the skin into the core, or it may “dimple” – a local buckling of the compression face on a honeycomb core, with a wavelength equal to the cell size of the core [11, 16]. The core can fail, usually in shear [17] but compression or tensile failure is also occur, or by local crushing. Then there is the bond between the face and the core: it can fail; and since resin adhesives are usually brittle, debonding is by brittle fracture [18]. Finally, the sandwich beam can fail by indentation of the faces and core at the loading point; but because this can be suppressed by distributing the load over an area about equal to the core section, it is easily avoided [2].

A substantial work has been performed on failure modes of foam-cored sandwich panels under static loading. For example, Allen [16] and Zenkert [19] have reviewed the basic failure modes in sandwich structures, Daniel *et al.* [20] have studied the failure modes in sandwich beams, Gdoutos *et al.* [21], have characterized the indentation failure and Gdoutos *et al.* [22] have reported on compression face wrinkling as well. Steeves and Fleck [23, 24] studied in detail the failure mechanisms in sandwich beam made of woven glass-epoxy skins and Divinycell PVC foam core under static loading.

The initiation, propagation and interaction of failure modes depend on the type of loading, constituent material properties and geometrical dimensions. The failure-mode maps of sandwich beams can provide useful information about the influence of different design parameters on the failure behavior of such components [25]. The failure mode maps describe the dominant mechanism, for a given design, which occurs at the lowest pressure. A transition in failure mechanism takes place when two mechanisms have the same failure load. This information [2] can be displayed as a diagram or map (Fig. 1).

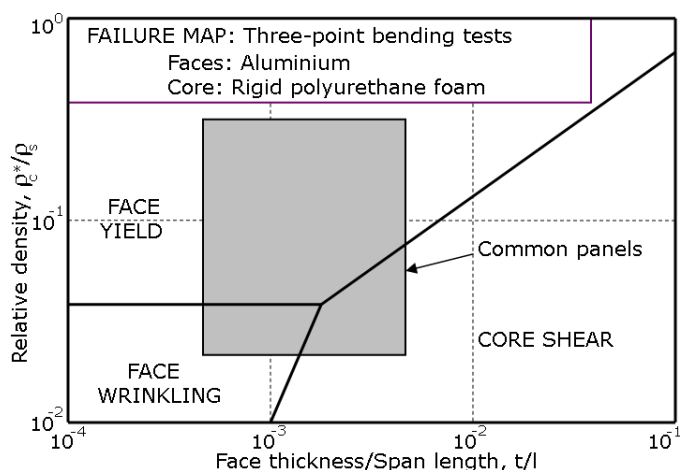


Fig. 1 – Failure-mode map of a sandwich panels.

The axes are the design parameters of the beam. The diagram is divided into fields; within one failure mechanism is dominant. The fields are separated by field boundaries, which are the loci of design points for which two mechanisms have the same failure load. We can see three failure modes dominate the map: face yielding, face wrinkling and core shear. At low values of t/l , the face fails by wrinkling if the core density is low and by yielding if the core density is high. As the face thickness increases, there is a transition from failure of the face to that of the core. For this loading configuration the core fails by yielding in shear [2].

3. EXPERIMENTAL INVESTIGATIONS

Failure mode of composite sandwich beams with different cores and different faces were investigated in the experimental program. Foams with 40 and 200 kg/m³ densities were used as core material, while Glass-Fibre Reinforced Polymer (GFRP), polyester, epoxy and aluminium are the faces materials. Three-point bending tests were carried out for sandwich beams. But in order to characterize these composite sandwich materials first was carried out a statistical analysis of the cellular structure for two different densities of the core material (40 and 200 kg/m³). After statistical analysis were performed static compression tests. These compression tests have had objective of determining main mechanical properties such as Young's modulus and yield stress. Results obtained from the static compression tests were used for the analytical determination of failure-mode maps of sandwich beams. Finally, the failure-mode maps were constructed for five considered sandwich types and validated by the experimental results.

3.1. STATISTICAL ANALYSIS

The microscopic distribution of the solid material within the cellular structure is governed by the cell geometry (shape and size) and the way the cells are packed.

The sandwich core morphology and cells dimensions for two different densities (40 and 200 kg/m³) were studied before testing through scanning electron microscopy (SEM), obtained with QUANTA FEG 250, that show a closed-cell foam configuration with cells generally elongated in the foam rise direction due to the foaming process and this gives an increase to mechanical anisotropy (Fig. 2). Measurement of the pores size was carried out with Sigma Scan Pro software.

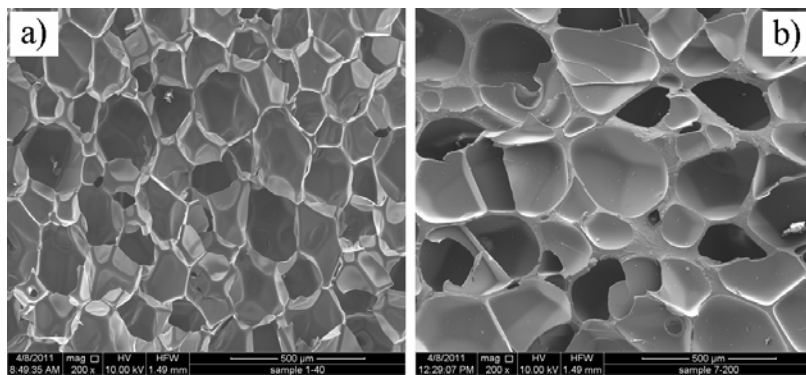


Fig. 2 – SEM images of used foams: a) 40 kg/m³ and b) 200 kg/m³.

Pore diameter versus frequency of pores histogram for polymeric foam with density of 40 kg/m³ is shown in Fig. 3a. The pores concentration is in the dimensional range of 93.1 μm and 277.6 μm and wall thickness varies between 1.05 μm and 2.9 μm. It can be easily seen that the highest concentration of pores for the lowest foam density was obtained in the range of 119.5 μm and 224.9 μm with a maximum concentration of pores in the domain of 172.2–198.6 μm (24.24 % frequency of pores diameter).

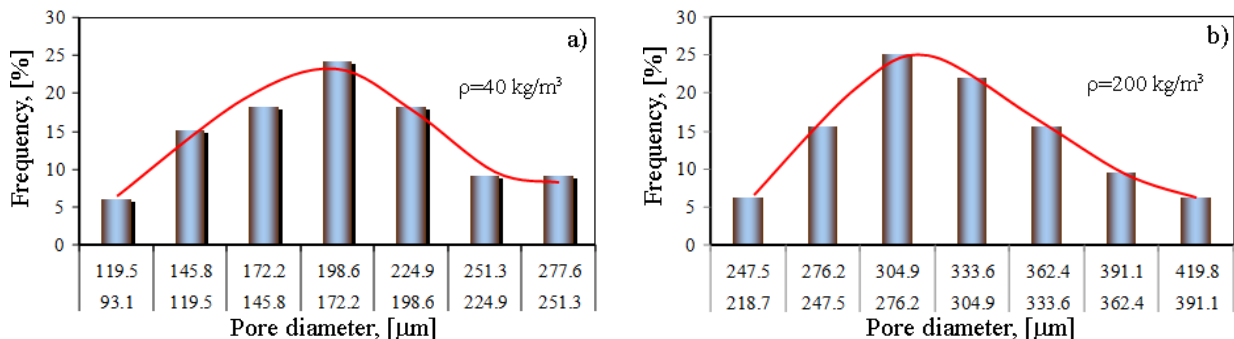


Fig. 3 – Pore distribution for PUR foams with closed cell structure.

Finally, for rigid foam with density of 200 kg/m^3 a pore diameter versus frequency of pores histogram is shown in Fig. 3b. In this case, the pores concentration is in the dimensional range of $218.7 \mu\text{m}$ and $419.8 \mu\text{m}$ and wall thickness varies between $6.5 \mu\text{m}$ and $26.1 \mu\text{m}$. Also, the highest concentration of pores for this density was obtained in the range of $247.5 \mu\text{m}$ and $362.4 \mu\text{m}$ with a maximum concentration of pores in the domain of $276.2\text{--}304.9 \mu\text{m}$ (25 % frequency of pores diameter).

For pore concentration investigation we used a reference surface with the area of 1.9072 mm^2 ($1.28 \text{ mm} \times 1.49 \text{ mm}$) at a magnitude of $200\times$. In order to obtain a better correlation of results were used the same geometrical parameters and magnitude for all densities [26].

3.2. COMPRESSION TESTS ON CORE MATERIALS

For plotting the failure-maps is needed to determine the main mechanical properties in compression of used foam core. Considering that the most applications of foams are under compressive loads, the study of properties such as Young's modulus and yield stress is very important. In this respect, the specimens used in the experimental program were in form of cubes ($12 \text{ mm} \times 12 \text{ mm} \times 12 \text{ mm}$).

Experimental compression tests were carried out on 10 kN Walter Bay testing machine at room temperature. The samples were subjected to a uniaxial compressive loading at a loading speed of 2 mm/min . For each type of test 5 specimens were used, and the tests were performed according with ASTM D1621-00 [27]. From data provided by the test machine, were drawn the typical compression stress-strain curves for both 40 and 200 kg/m^3 densities (Fig. 4).

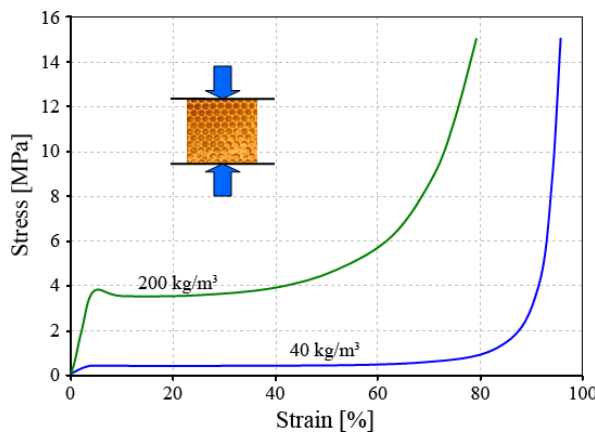


Fig. 4 – Typical stress-strain curves. Effect of density.

On the recorded stress-strain curves [28] the following regions can be identified: the first part of the curve shows linear-elastic behavior up to yield (up to 5 %), a small softening in stress after yield, a plateau after yield (between 10–60 %), and in the end there is an increase in stress, called densification (above 60% strain).

After processing of data was obtain a value of the Young's modulus equal to 4.2 MPa for foam with 40 kg/m^3 density, respectively a value of 122 MPa for foam with 200 kg/m^3 density. Also, yield stress values obtained were 0.38 MPa for the lowest foam density, respectively 4.14 MPa for the higher foam density. The results presented above indicating an increase of the mechanical properties with increasing of density, which means that the density plays a major role in determining the compressive behaviour of foams.

Statistical analysis presented above, determination of static compression behaviour, respectively mechanical properties of foams will be used in plotting of failure-mode maps.

3.3. THREE-POINT BENDING TESTS OF SANDWICH BEAMS

The three-point bending tests were performed on 5 kN Zwick/Roell 005 tensile/compression testing machine, according to ASTM C393-00 [29].

Flexural tests on sandwich specimens were conducted at room temperature in displacement control at a crosshead speed of 2 mm/min. Five samples were tested for each type of sandwich beam and as it can be seen in Fig. 2 the sandwich beams presents the following in plane dimensions: span of the beam, l , high, h , width, b , face thickness, t and core thickness, c . Also, d is distance between centroids of faces and L_{tot} is total length of the beam.

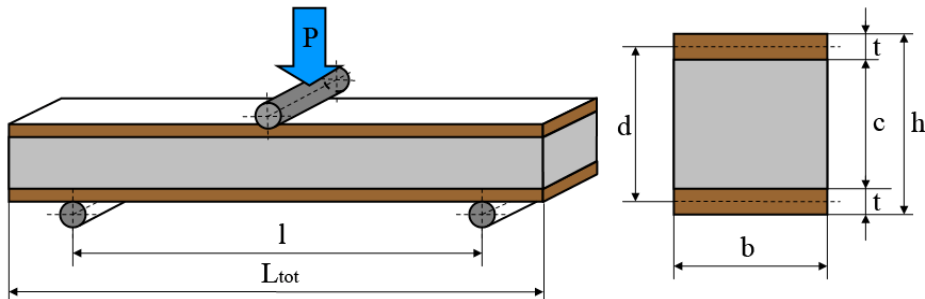


Fig. 5 – Sandwich beam loaded in three-point bending.

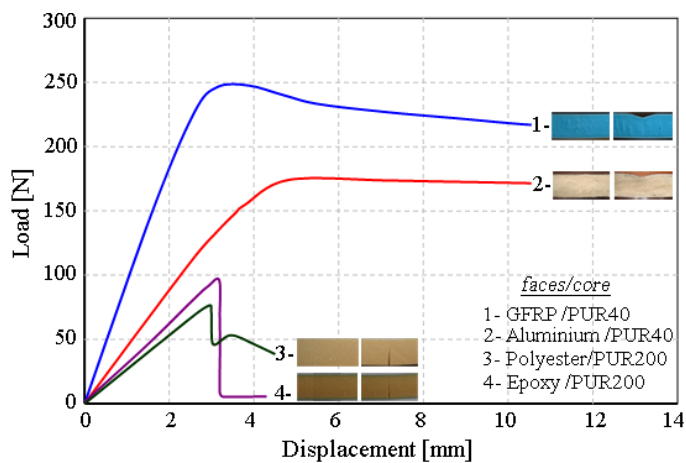


Fig. 6 – Load-displacement curves of used sandwich beams under 3PB.

Based on previous considerations, in this paper we determined a failure maps for sandwich beams with: aluminium faces with polymeric foam core ($\rho = 40 \text{ kg/m}^3$), glass-fiber reinforced polymer (GFRP) faces (with different thickness) with polymeric foam core ($\rho = 40 \text{ kg/m}^3$ and 200 kg/m^3), epoxy faces with polymeric foam core ($\rho = 200 \text{ kg/m}^3$) and polyester faces with foam core ($\rho = 200 \text{ kg/m}^3$), loaded in 3PB, as in Fig. 5. The bonding between the faces and core material of sandwich structures was assumed to be perfect.

Typical load-displacement curves of tested beams obtained from the experimental tests are presented in Fig. 6, while the material properties, geometrical parameters and flexural test results of the considered sandwich beams are listed in Table 1 and Table 2.

Table 1
Material properties of the sandwich beam

Sandwich Type		Density [kg/m^3]			Young's modulus [MPa]			Yield strength [MPa]		
Face	Core	ρ_f	ρ_c	ρ_s	E_f	E_c	E_s	σ_{vf}	σ_{vc}	σ_{vs}
Aluminum, [30]	PUR40	2705	40	1170	69000	4.2	1600	78	0.38	53.4
GFRP [31]		1200			9000			106		
GFRP [31]	PUR200	1200	200	122	9000	122	4.14	106	4.14	53.4
Epoxy [2]		1060			3790			60		
Polyester [2]		1150			4730			50		

Table 2

The geometrical parameters and flexural test results of the sandwich beams

Sandwich type		Geometrical parameters						Failure load	
Face	Core	l [mm]	t [mm]	t/l	c [mm]	b [mm]	d [mm]	F_{max} [N]	F_{cr} [N]
GFRP	Foam	150	1.10	0.0073	21.80	51.60	22.90	225.87	153.43
		200		0.0055		49.40		186.65	132.67
		70	1.30	0.0186	20.90	50.00	22.20	329.49	254.55
		150		0.0087		50.00		288.86	222.86
		200		0.0065		50.20		261.25	188.58
		70	1.40	0.0200	21.40	51.40	22.80	412.34	232.84
		150		0.0093		49.70		304.11	166.22
		70	1.50	0.0214	20.50	51.30	22.00	442.10	277.23
		150		0.0100		50.50		431.16	266.33
		200		0.0075		50.00		377.80	265.15
		70	1.60	0.0229	21.20	51.10	22.80	376.35	199.25
		150		0.0107		49.70		262.92	114.48
		200		0.0080		50.10		224.69	86.12
		70	2.00	0.0286	13.60	33.20	15.60	3155.16	2121.61
		120		0.0167		32.00		2430.91	1651.56
Epoxy		40	0.17	0.0043	12.30	12.30	12.47	207.72	150.41
		90		0.0019	11.86	12.20	12.03	92.74	82.12
Polyester		40	0.10	0.0025	12.30	12.30	12.40	201.47	145.25
		90		0.0011	11.90	12.20	12.00	88.21	78.36
Aluminum		70	0.40	0.0057	26.40	48.80	26.80	241.76	185.85
		150		0.0027		48.40		195.07	149.59
		200		0.0020		48.00		173.01	133.86

Figure 7 presents the load-displacement curve for determining the corresponding critical load, F_{cr} and maximum load, F_{max} for a sandwich beam with GFRP faces ($t = 1.3$ mm) and foam core ($\rho = 40 \text{ kg/m}^3$).

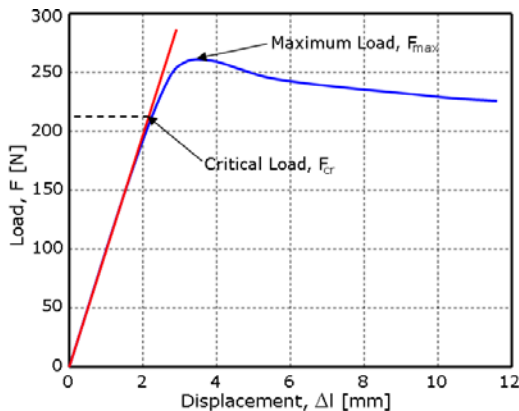


Fig. 7 – A typical load-displacement curve for determining the corresponding critical load.

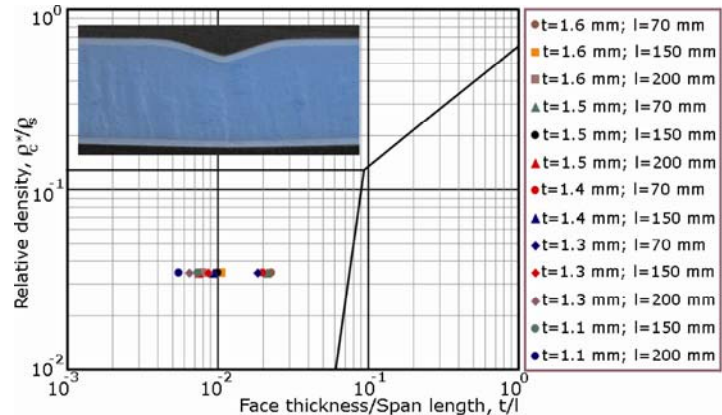


Fig. 8 – A failure mode map for a rectangular sandwich beam with GFRP faces and rigid PUR foam core (40 kg/m^3 density).

Using the failure equations and material properties presented we can now develop failure mode maps for these composite sandwich beams. The failure mode maps indicate graphically the expected failure mode for possible sandwich beam by showing the boundaries between the different failure modes [25, 32]. The maps plot the core relative density, ρ_c/ρ_s as a function of the face thickness/span length, t/l . A failure mode map was constructed for each material combination and the corresponding values for the tested specimens are also plotted as different markers, considering geometry and span of the sandwich beams.

In Figs. 8–12 are plotted the failure mode map for used rectangular sandwich beam with different faces and rigid polyurethane foam core (40 and 200 kg/m^3 density), loaded in three points bending. The beams had different values of t/l in range of 0.0011 and 0.0286.

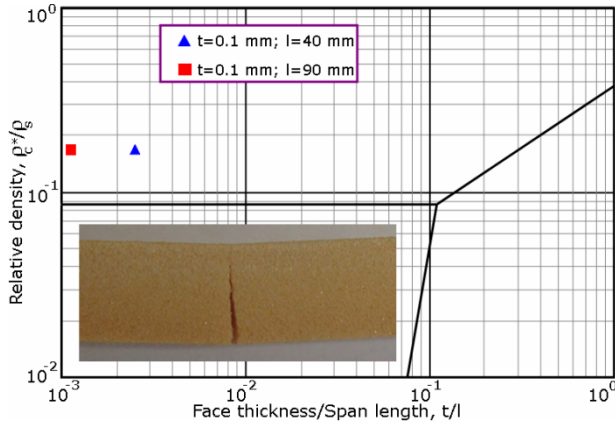


Fig. 9 – A failure mode map for a sandwich beam with polyester faces and rigid PUR foam core (200 kg/m^3 density).

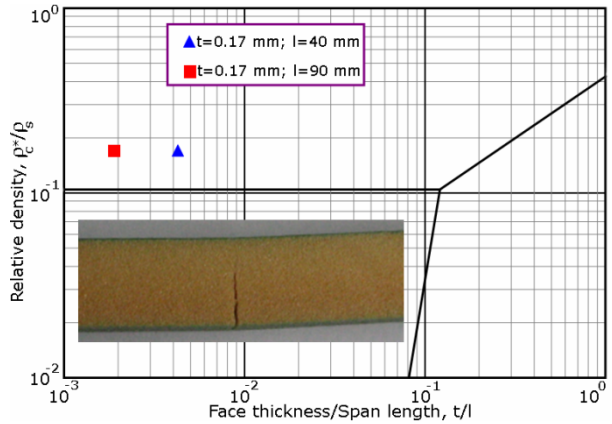


Fig. 10 – A failure mode map for a sandwich beam with epoxy faces and rigid PUR foam core (200 kg/m^3 density).

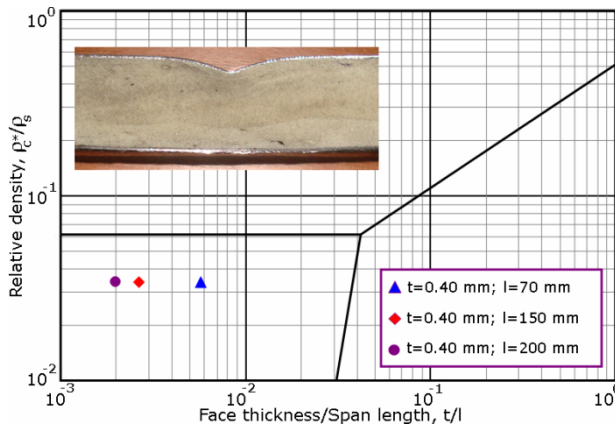


Fig. 11 – A failure mode map for a sandwich beam with aluminum faces and rigid PUR foam core (40 kg/m^3 density).

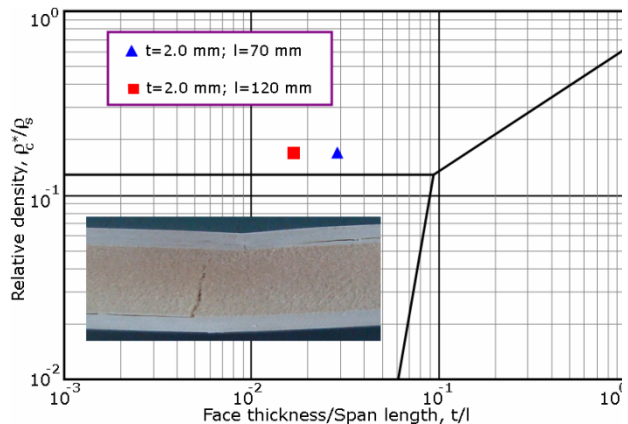


Fig. 12 – A failure mode map for a sandwich beam with GFRP faces and rigid PUR foam core (200 kg/m^3 density).

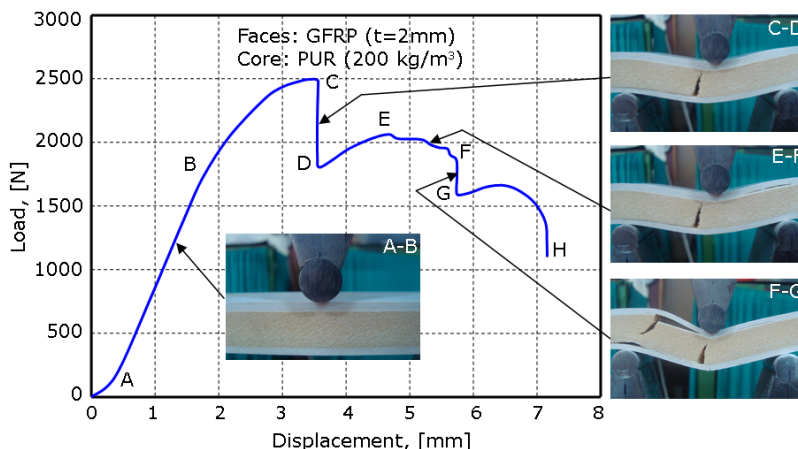


Fig. 13 – Typical load-displacement curves of sandwich beam under 3PB.

From all of these figures (Figs. 8–12) it can be easily seen a good agreement between the observed (experimental) and expected (analytical) mechanism of failure.

In Fig. 13 is presented the typical load-displacement curves from the experimental tests for sandwich beam with GFRP faces (2 mm thickness) and rigid polyurethane foam core (200 kg/m^3 density). In this case we can observe following zones: a linear-elastic zone (A – B), where B point represent a critical force and is determined in Figure 7; after this zone appear a face yielding (B – C), followed by core shearing (C – D);

after this zone, load increase slowly (D – E), until appear a new core shear, (E – F); and finally appear the ultimate failure. In the same figure is presented the specimen after load. Failure (critical) load was defined as first pronounced deviation from the linearity in the loading curve [2].

4. CONCLUSIONS

This paper presents failure-mode maps for sandwich beams with different faces and core materials. Each failure mode map is for a group of beam designs, the face sheets properties and the type of core are specified but the geometry and core density may vary. The failure diagrams are useful tools to predict the failure mode of these materials based on core density and dimensions of the considered sandwich structure (beam or panel). It may be drawn the following conclusions:

- The sandwich core morphology and cells dimensions for two different densities (40 and 200 kg/m^3) were studied before testing through scanning electron microscopy (SEM) that showing a closed-cell foam configuration with cells generally elongated in the foam rise direction due to the foaming process and this gives an increase to mechanical anisotropy (Fig. 2). The highest concentration of pores for the lowest foam density was obtained in the range of $119.5 \mu\text{m}$ and $224.9 \mu\text{m}$ with a maximum concentration of pores in the domain of 172.2 – $198.6 \mu\text{m}$ (24.24 % frequency of pores diameter). Also, the highest concentration of pores for 200 kg/m^3 foam density was obtained in the range of $247.5 \mu\text{m}$ and $362.4 \mu\text{m}$ with a maximum concentration of pores in the domain of 276.2 – $304.9 \mu\text{m}$ (25 % frequency of pores diameter).
- For plotting of failure-maps have been determined the main mechanical properties in compression of core material. In this case there was obtained a value of the Young's modulus equal to 4.2 MPa for foam with 40 kg/m^3 density, respectively a value of 122 MPa for 200 kg/m^3 foam density. Also, yield stress values obtained were 0.38 MPa for the lowest foam density, respectively 4.14 MPa for the higher foam density. The results presented above indicating an increase of the mechanical properties with increasing of density, which means that the density plays a major role in determining the compressive behaviour of foams.
- For sandwich beams with: polyester faces and foam core, epoxy faces and foam core, and GFRP faces with foam cores (foam core with 200 kg/m^3 density), the failure mode observed during tests was face failure, and was in agreement with the failure mode resulted from the failure map, (Figs. 9, 10 and 12).
- Also, two types of sandwiches: aluminium face ($t = 0.4 \text{ mm}$) with foam core (40 kg/m^3), and GFRP faces with foam core (40 kg/m^3), the failure mode observed on the tests was face wrinkling, and was in agreement with the failure mode resulted from the failure map, (Figs. 8 and 11).

All of these diagrams are useful to describe the damage mechanics of the composite sandwich beams, (Fig. 13), and as a general conclusion it can be easily observed that all failure modes predicted by the failure mode maps were experimentally validated using static three-point bending tests.

ACKNOWLEDGMENTS

This work was partially supported by the strategic grant POSDRU/159/1.5/S/137070 (2014) of the Ministry of National Education, Romania, co-financed by the European Social Fund – Investing in People, within the Sectoral Operational Programme Human Resources Development 2007-2013. Experimental tests were performed in the facilities of the CNCS – UEFISCDI Grant PN-II-ID-PCE-2011-3-0456, contract number 172/2011.

REFERENCES

1. TRIANTAFILLOU T.C., *Failure mode maps and minimum weight design for structural sandwich beams with rigid foam cores*, Diploma in Civil Engineering, Greece, 1985.
2. GIBSON L.J., ASHBY M.F., *Cellular Solids-Structures and properties-Second edition*, Press Syndicate, University of Cambridge, 1997.

3. SCUDAMORE R.J., CANTWELL W.J., *The effect of moisture and loading rate on the interfacial fracture properties of sandwich structures*, Polymer Composite, **23**, pp. 406-417, 2002.
4. MIRZAPOUR A., BEHESHTY M.H., VAFAYAN M., *The response of sandwich panels with rigid polyurethane foam cores under flexural loading*, Iranian Polymer Journal, **14**, pp. 1082-1088, 2005.
5. YOSHII A., *Optimum design of advanced sandwich composite using foam core*, Adv. Comp. Mat., **2**, pp. 289-305, 1992.
6. THOMSEN O.T., *Theoretical and experimental investigation of local load bending effects in sandwich plates*, Composite Structures, **30**, pp. 85-101, 1995.
7. ZENKERT D., HALLSTROM S., SHIPSHA A., *Design aspects of marine structures*, Maryland University, 1999, pp. 28-32.
8. BIRSAN M., SADOWSKI T., MARSAVINA L., LINUL E., PIETRAS D., *Mechanical behavior of sandwich composite beams made of foams and functionally graded materials*, International Journal of Solids and Structures, **50**, pp. 519-530, 2013.
9. LEE C.S., LEE D.G., *Co-cure method for foam sandwich composite manufacture*, Composite Structures, **66**, pp. 231-238, 2004.
10. JONGMAN K., STEPHEN R., *Design of sandwich structures for concentrated loading*, Comp. Structures, **59**, 365-373, 2001.
11. KUENZI E.W., *Minimum weight structural sandwich*, Forest Products Laboratory, Madison WI, 1965.
12. UENG C.E.S., LIU T.L., *Least weight of a sandwich panel*, in R.R. Craig (ed.), New York, 1979, pp. 41-44.
13. FROUD G.R., *Your sandwich order, Sir?* Composites, **11**, 3, pp. 133-138, 1980.
14. TRIANTAFILLOU T.C., GIBSON L.J., *Failure mode maps for foam core sandwich beams*, Mat. Sci. Eng., **95**, pp. 37-53, 1987a.
15. TRIANTAFILLOU T.C., GIBSON L.J., *Minimum weight of foam core sandwich panels for a given strength*, Mat. Sci. Eng., **95**, pp. 55-62, 1987b.
16. ALLEN H.G., *Analysis and Design of Structural Sandwich Panels*, Pergamon Press, Oxford, UK, 1969.
17. HALL D.J., ROBSON B.L., *A review of the design and materials evaluation programmed for the GRP/foam sandwich composite hull of the RAN mine hunter*, Composites, **15**, pp. 266-276, 1984.
18. HONG C.S., JEONG K.Y., *Stress intensity factors in anisotropic sandwich plate with a part-through crack under mixed mode deformation*, Eng. Fract. Mech., **21**, pp. 285-292, 1985.
19. ZENKERT D., *An introduction to Sandwich Construction*, Chameleon, London, 1995.
20. DANIEL I.M., GDOUTOS E.E., WANG K.A., ABBOT J.L., *Failure modes of composite sandwich beams*, Int. J. of Dam. Mech., **11**, pp. 309-334, 2002.
21. GDOUTOS E.E., DANIEL I.M., WANG K.A., *Indentation failure in composite sandwich structures*, Exp. Mech., **42**, pp. 426-431, 2002.
22. GDOUTOS E.E., DANIEL I.M., WANG K.A., *Compression facing wrinkling of composite sandwich structures*, Mech. of Mat., **35**, pp. 511-522, 2003.
23. STEEVES C.A., FLECK N.A., *Collapse mechanisms of sandwich beams with composite faces and a foam core, loaded in three-point bending. Part I: Analytical models and minimum weight design*, Int. J. of Mech. Sci., **46**, pp. 461-583, 2004.
24. STEEVES C.A., FLECK N.A., *Collapse mechanisms of sandwich beams with composite faces and a foam core, loaded in three-point bending. Part II: Experimental investigation and numerical modeling*, Int. J. of Mech. Sci., **46**, pp. 585-608, 2004.
25. ANDREWS E.V., MOUSSA N.A., *Failure mode maps for composite sandwich panels subjected to air blast loading*, Int. J. of Imp. Eng., **36**, pp. 418-425, 2009.
26. LINUL E., MARSAVINA L., VOICONI T., SADOWSKI T., *Study of factors influencing the mechanical properties of polyurethane foams under dynamic compression*, J. of Physics: Conf. Series, **451**, pp. 1-6, 2013.
27. ***, ASTM D1621, *Standard Test Method for Compressive Properties of Rigid Cellular Plastics*, 2000.
28. MARSAVINA L., LINUL E., VOICONI T., SADOWSKI T., *A comparison between dynamic and static fracture toughness of polyurethane foams*, Pol. Test., **32**, pp. 673-680, 2013.
29. ***, ASTM C393, *Standard Test Methods for Flexural Properties of Sandwich Constructions*, 2000.
30. ***, www.matweb.com
31. CONSTANTINESCU D.M., FAUR N., MARSAVINA L., ALEXANDRESCU E., *Refinement on the testing and behaviour of composite materials used in aerospace industry*, Proceedings of the “Excellence Research as a way to ERA” (CD ROM) 202, pp. 1-6, 2007.
32. LIM T. S., LEE C.S., LEE D.G., *Failure modes of foam core sandwich beams under static and impact loading*, J. of Comp. Mat., **38**, pp. 1639-1662, 2004.

Received September 22, 2014